ACS Sustainable Chemistry & Engineering

pubs.acs.org/journal/ascecg

Research Article

Novel and Efficient Biotechnological Approach to Produce 2,5-Diformylfuran from Biomass-Derived 5-Hydroxymethylfurfural

Alberto Millán Acosta,* Clara Cuesta Turull, Diana Cosovanu, Núria Sala Martí, and Ramon Canela-Garayoa*

Cite This: *ACS Sustainable Chem. Eng.* 2021, 9, 14550−14558

Read Online

ACCESS | Metrics & More | Article Recommendations | Supporting Information

ABSTRACT: The preparation of compounds of interest from biomass-derived 5-hydroxymethylfurfural (HMF) has attracted considerable attention. One such compound is 2,5-diformylfuran (DFF), obtained through oxidation of the hydroxyl group of HMF. Herein, we describe for the first time the whole-cell oxidation of HMF to DFF by *Fusarium culmorum* EAN 51. Although the chemocatalytic transformation of HMF into DFF has been widely studied, biocatalytic processes have been scarcely reported and are limited to enzymatic synthesis using the combination of several enzymes. The whole-cell transformation of HMF into DFF is preferable thanks to the inherent presence of the different enzymes, significantly reducing the cost of the process. *F. culmorum* showed a high capability to reduce to 2,5-di(hydroxymethyl)furan (DHMF) and oxidize to DFF the substrate with high yields depending on the nitrogen source and the concentration of peptone and glucose in the media, which highly affected the redox capability of this strain. After careful optimization of the concentration of both nutrients through response surface methodology, 50 mM HMF were transformed into DFF with a high yield (92%) and selectivity (94%). These results open a new line of investigation in the sustainable production of DFF from renewable biobased resources.

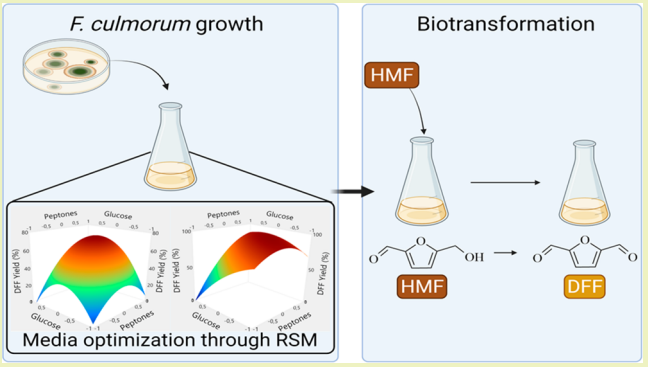

KEYWORDS: *Biotransformation, RSM, Fusarium culmorum, Biocatalysis, HMF, DFF*

INTRODUCTION

The dependence on fossil resources to prepare chemical building blocks is a concern that manifests the need for greener chemistry based on new sustainable production pathways from renewable biobased resources. Lignocellulosic biomass, which is abundant as waste, can be transformed into several compounds of commercial interest.[1] One such compound is 5-hydroxymethylfurfural (HMF), a platform chemical obtained through dehydration of sugars present in lignocellulosic material. It is considered one of the "Top 10 + 4" list of biobased chemicals according to the U.S. Department of Energy (DOE).[2] The presence of one aldehyde group and one hydroxyl group allows the preparation of different value-added derivatives such as 2,5-di(hydroxymethyl)furan (DHMF), 2,5-diformylfuran (DFF), 5-hydroxymethyl-2-furancarboxylic acid (HMFCA), 5-formyl-2-furancarboxylic (FFCA) acid, and 2,5-furandicarboxylic acid (FDCA) through oxidation/reduction reactions. The market value of these compounds is higher than that of HMF, and for this reason, it is considered an excellent intermediate between biomass waste and biochemicals.[3] DFF results from the oxidation of the hydroxyl group present in HMF, and therefore, it contains two symmetrical aldehyde groups. It is a precursor with applications in the synthesis of polymers, fluorescent materials, and therapeutics, among others,[4−8] and it may be an interesting building block for the preparation of biobased polyurethane thermosets.[9]

The synthesis of DFF has been carried out by using chemical catalysis.[2,10] Yan et al. catalyzed the selective oxidation of HMF to DFF at 130 °C and 3 MPa O_2 with high conversion (93.7%) and selectivity (94.5%) using nanobelt-arrayed vanadium oxide hierarchical microspheres.[11] Later, a DFF yield of 99% was achieved at 120 °C and 20 mL/min O_2 starting from HMF using highly active and robust vanadium dioxide-embedded mesoporous carbon spheres.[12] The chemocatalytic synthesis of DFF has also been studied starting from fructose by dehydration to HMF and selective oxidation to DFF. Zhao et al. achieved a DFF yield of 77% at 150 °C and 20 mL/min O_2 using a series of protonated molybdenum trioxide and nitrogen-doped carbon bifunctional catalysts.[13] Further, the catalyst could be recovered and reused without significant loss of activity. Recently, carbon nanoplates synthesized by a

Received: August 5, 2021
Revised: September 10, 2021
Published: October 18, 2021

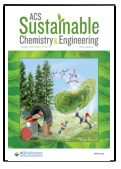

molten-salt method showed a DFF yield of 70.3% in a one-pot and one-step conversion of fructose to DFF performed at 140 °C using oxygen as the only oxidant.[14]

Although the recent results obtained by chemocatalytic methods are promising and encouraging, biocatalytic preparation is an attractive alternative thanks to its advantages such as milder reaction conditions, no need for high-cost chemicals as many of the chemical processes, and higher selectivity.[8] Nonetheless, reports in the literature are scarce. The enzymatic oxidation of HMF to DFF via galactose oxidase (GO), catalase, and horseradish peroxidase (HRP) has been reported with almost quantitative yields within 96 h for a concentration of HMF of 30 mM.[15] The main drawbacks of this study were that the use of these three enzymes added a high cost to the process, and the DFF productivity was low, considering the long reaction time needed. Later, Wu et al. immobilized the same three enzymes into $Cu_3(PO_4)_2$ nanoflowers, which allowed a higher concentration of substrate (200 mM) while keeping high yields, although the reaction times were still long (168 h), leading to a low productivity.[16] Recently, the fungal enzymes glyoxal oxidase (MtGLOx)[17] and aryl alcohol oxidase (CgrAAO)[18] have shown good preliminary results in the catalytic synthesis of DFF from HMF starting from low concentrations of substrate (≤20 mM). Although promising results have been obtained by enzymatic catalysis, the low concentrations of substrate and productivities obtained call for more research. Furthermore, the whole-cell transformation of HMF into DFF has not been described. Whole cells offer advantages in the biocatalytic upgrade of HMF because they are low priced, more stable, provide a protective environment to enzymes, and have no need for separation and purification of the enzymes.[4,19,20] Specifically, in the HMF oxidation to DFF, the whole-cell transformation is of great interest due to the need to combine different enzymes for efficient oxidation. The use of a single whole-cell catalyst would reduce the cost of the process thanks to the inherent presence of all the enzymes required. Moreover, whole cells allow the implementation of hybrid processes combining microbial and enzyme catalysis, which may be promising in the valorization of compounds such HMF.[21]

The biggest challenge for the whole-cell transformation of HMF is its high toxicity toward microorganisms, and more research is needed to advance toward the valorization of HMF in this regard.[4,8] *Fusarium* species have proven to be good biocatalysts for the transformation of HMF due to their high tolerance toward high HMF concentrations using a low inoculum size,[22] and some *Fusarium* species are natural producers of the enzyme GO,[23,24] the catalyst of the oxidation of HMF to DFF, as mentioned above. Therefore, *Fusarium* species are promising candidates for the whole-cell oxidation of HMF to DFF. Moreover, the recovery of polysaccharides with immunomodulatory and antioxidant properties from *Fusarium* after the biotransformation would assist in integrating the process in the circular economy.[25] Furthermore, products obtained through biotransformation using *Fusarium* can be labeled as "natural".[26]

Response surface methodology is an experimental technique widely used to find the optimum conditions for a process. It consists of the use of mathematical optimization techniques to evaluate the relationship between a set of variables and one or more responses, and it is based on the sequential design and analysis of experiments.[27,28] Commonly, a first-order design (such as a factorial design) is first assessed, and a linear model is fit. It is possible to use widespread data points at this stage to get an overview of the design space.[29] When evidence of curvature is found (with techniques like the path of the steepest ascent or the addition of central points to the factorial design[30]), a second-order design (such as a central composite design (CCD)) can be built from the initial or a new factorial design by the addition of axial points. This allows the fit of a quadratic model that, ideally, will locate a region of interest within the design space where the process is improved.[29−31] However, this is not the only possibility, and different experimental approaches are described, such as performing a new CCD experiment in each optimization step by discarding parts of the design space that give suboptimal responses (adaptive RSM) or centrally building a new design space around each successive optimum (successive RSM).[27] RSM presents several advantages in medium optimization compared to traditional methodologies such as one factor at a time (OFAT), which is based on performing changes of one variable at a time while keeping others constant at fixed values. More information (such as interactions among the variables) can be obtained with fewer experiments, time, and materials.[28,32]

The capability of *F. culmorum* EAN51 to biotransform HMF into an unknown compound was previously reported in a screening of different *Fusarium* species.[22] This compound was further identified as DFF; however, the yield and selectivity obtained were low and far from optimal. In this work, the capability of this fungus to produce DFF is assessed by evaluating the effect of different nitrogen sources and through optimization of the concentration of peptone and glucose in the culture medium through RSM.

EXPERIMENTAL SECTION

Materials. *F. culmorum* EAN 51 (UdL-TA-3.237) was obtained from the Spanish Type Culture Collection (CECT2148). HMF (98%) was purchased from Fluorochem Ltd. (Hadfield, UK). DHMF (97%) was purchased from Apollo Scientific (Stockport, UK). DFF (97%), ethyl acetate, casein hydrolysate, and glucose were purchased from Sigma-Aldrich (Missouri, USA). Malt extract was purchased from Condalab (Madrid, Spain). Peptone digest of meat was purchased from Biokar (Barcelona, Spain). Peptone from soybean was purchased from Acros Organics (Pittsburgh, PA, USA).

Cultivation of *F. culmorum*. *F. culmorum* was maintained by replications on malt extract agar (MEA: 20 g/L of malt extract, 20 g/L of glucose, 1 g/L of peptone from soybean, 15 g/L of agar) at 4 °C. Before biotransformation experiments, it was activated in MEA for 7 days in the dark at 28 °C.

Selection of Nitrogen Source. The activated strain of *F. culmorum* was inoculated into flasks containing 15 mL of MES (20 g/L of malt extract, 20 g/L of glucose, 9 g/L of peptone from soybean), MEM (20 g/L of malt extract, 20 g/L of glucose, 9 g/L of peptone from meat), or MEC (20 g/L of malt extract, 20 g/L of glucose, 9 g/L of peptone from casein) by the addition of three fungal discs of 8 mm taken from the solid MEA medium. The pH of the media was 5.25. The flasks were incubated in a rotatory shaker in the dark at 28 °C and 160 rpm. After 3 days, HMF was added to the media at a concentration of 50 mM. Analyses were performed 72 h after the HMF addition.

Optimization of Glucose and Peptone Concentrations. The activated strain of *F. culmorum* was inoculated into flasks containing 15 mL of MEC containing different concentrations of glucose and peptones by adding three fungal discs of 8 mm taken from the solid MEA medium. The pH of the media was 5.25. The flasks were incubated in a rotatory shaker in the dark at 28 °C and 160 rpm. After 3 days, HMF was added to the media at a concentration of 50 mM.

https://doi.org/10.1021/acssuschemeng.1c05308
ACS Sustainable Chem. Eng. 2021, 9, 14550−14558

Table 1. First and Second Central Composite Designs

	Levels									
	First CCD					Second CCD				
Factors	$-\alpha$ (−1.41)	−1	0	1	α (1.41)	$-\alpha$ (−1.41)	−1	0	1	α (1.41)
[Peptone] (g/L)	0.5	3	9	15	17.5	6.3	7.5	10.5	13.5	14.7
[Glucose] (g/L)	0.20	6	20	34	39.8	14.9	17	22	27	29.1

Response Surface Methodology. Two successive central composite designs were built for the optimization of the glucose and peptone concentration in the media. The experimental conditions of both models are shown in Table 1. The two-factor central composite designs were developed starting from 2^2 factorial points, adding a central point performed in quintuplicate, and finally adding four axial points (α = 1.41). The response for both models was the maximum DFF yield obtained within 48 h of reaction.

The full second-order model in terms of the coded variables is

$$Y = \beta_0 + \beta_1 x_1 + \beta_2 x_2 + \beta_{11} x_1^2 + \beta_{22} x_2^2 + \beta_{12} x_1 x_2 \quad (1)$$

where Y represents the parameter to be modeled (DFF yield), β_0 a constant coefficient, β_1 and β_2 the regression coefficients for linear effects, β_{11} and β_{22} the regression coefficients for quadratic effects, β_{12} the regression coefficient for the interaction effect, and x_1 and x_2 the independent coded variables ([peptone] and [glucose], respectively).

The model was validated by running independent assays at the optimum conditions in triplicate and at different points within the design space in duplicate.

GC-FID Analysis. Aqueous aliquots were withdrawn from the reaction broth at selected reaction times. The compounds were extracted from the aqueous aliquots using ethyl acetate. GC-FID analyses were performed with an Agilent 7890 GC (Agilent Technologies, Palo Alto, CA, USA) with an ultrainert splitless liner containing a piece of glass wool coupled to an FID detector. For the chromatographic separation, an FFAP (30 m × 0.25 mm i.d.; 0.25 μm film thickness) column from Agilent was used at a constant flow of 1 mL/min using hydrogen as the carrier gas. The injector temperature was 230 °C, and the oven program was from 100 °C (held for 1 min) to 240 °C at 20 °C/min (held for 5 min). Calibration curves were performed periodically for the quantification of the compounds.

Determination of Amino Acid Profile by UHPLC. The amino acid contents of the samples were determined on freeze-dried and pulverized tissue. Acidic hydrolysis of the sample (50 mg) was carried out using 5 mL of 6 N HCl (110 °C, overnight, under N_2).[33,34] Hydrolysis tubes were cooled and centrifuged at 3000g for 30 min to remove particulate matter. Aliquots of 25 μL of hydrolysate were evaporated using a SpeedVac and reconstituted in 500 μL of water:acetonitrile (20:80, v/v). Samples were filtered through a 0.22 μm hydrophilic polytetrafluoroethylene (PTFE) membrane before injection. The injection volume was 5 μL.

Quantitation of individual amino acids was performed using a method described by Guo et al. with modifications.[35] UHPLC was performed using a Waters Acquity system equipped with a BEH Amide column (2.1 mm × 150 mm; 1.7 μm). The mobile phase consisted of solvent A (10 mM ammonium formate in water with 0.15% formic acid) and solvent B (ammonium formate-saturated acetonitrile with 0.15% formic acid). The gradient elution followed was 15% A and 85% B maintained for 3 min at 0.5 mL/min, then from 15% to 20% A in 3 min, from 20% to 24% A in 1.5 min, from 24% to 60% A at 0.6 mL/min in 1.5 min, and maintained for 3 min. Finally, initial conditions were regained in 2 min. The flow rate of the mobile phase was 0.5 mL/min, and the column temperature was maintained at 30 °C. The column was cleaned with weak (20% acetonitrile) and strong (80% acetonitrile) washing solvents between injections.

Detection and quantitation of amino acids in the hydrolysate were performed by using a multiple reaction monitoring method (MRM) in a triple quadrupole detector (TQD) mass spectrometer. The system was equipped with an electrospray ionization (ESI) source operated in positive ion mode. Parameters in the source were set as described in the bibliography.[35]

Statistical Analysis. The statistical analyses were assessed using the software JMP Pro 14 (SAS). The results obtained were subjected to analysis of variance (ANOVA). Statistical significance was assessed with the p-value in Fisher's test with a 95% confidence level. The assumption of normality was tested using Shapiro–Wilk normality test.

Recovery of DFF from Reaction Media. The biotransformation broth was extracted three times with ethyl acetate. The organic extracts were dried over Na_2SO_4 anhydrous. Then, they were filtrated and evaporated to dryness. The purity of the crude reaction product was assessed by NMR.

RESULTS AND DISCUSSION

Effect of Nitrogen Source. The selection of adequate nitrogen and carbon sources and the concentration of both nutrients in the media can significantly improve the yields and productivities of biocatalytic processes when working with whole cells.[32] Filamentous fungi require organic compounds as carbon and energy sources due to their heterotrophic nature. Sugars are the preferred carbon source for the growth of the cells because they are easily incorporated into the microorganism metabolism. Among them, glucose is one of the most common ingredients of microbial media;[36] it is crucial for the biotransformation of HMF by *Fusarium* species[22] and has proven to be a good carbon source for the production of GO by *Fusarium* species.[37] Therefore, it was selected as the carbon source. The preferred nitrogen source, however, is not as evident and highly depends on the microorganism and the process studied. Nitrogen may be added to the media as inorganic compounds, such as ammonia or nitrate, or as organic compounds, such as peptones or free amino acids, and it plays a crucial role in the metabolite and enzyme production of the cells.[38] The effect of the nitrogen source was assessed by studying the influence of three different peptones (soybean, meat, and casein) over the HMF transformation (Figure 1).

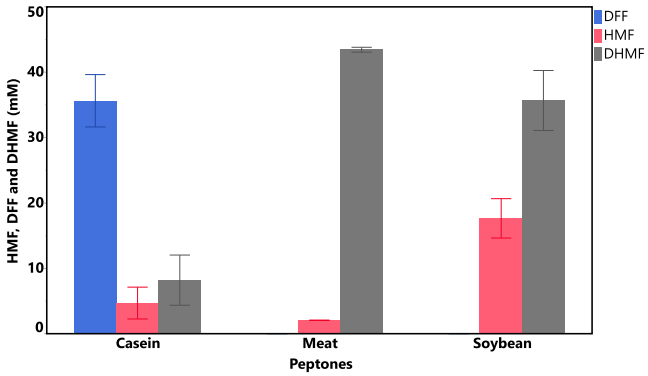

Figure 1. Effect of nitrogen source on HMF transformation. Conditions: 50 mM HMF; 15 mL of MEM, MES, or MEC medium; three discs of biocatalyst; pH 5.25; 160 rpm; 28 °C; and 72 h.

https://doi.org/10.1021/acssuschemeng.1c05308
ACS Sustainable Chem. Eng. 2021, 9, 14550−14558

When soybean or meat peptones were added to the media, HMF was exclusively reduced to 2,5-di(hydroxymethyl)furan (DHMF), a process reported using whole cells as biocatalysts.[22,39−41] However, when peptone from casein was added to the media, both DHMF and DFF were produced and identified in the reaction broth. This indicated that the oxidative process was favored when peptone from casein was used as a nitrogen source under the conditions studied. However, the DFF yield (70%) and selectivity (80%) were not optimal. Moreover, HMF was not wholly transformed. For these reasons, peptone from casein was selected for further optimization.

The production, secretion, and maturation of GO, the enzyme likely involved in the oxidation of HMF to DFF by *F. culmorum*, is a complex process that requires several steps and cofactors.[23] The effect of the different peptones on the redox capability of *F. culmorum* may be attributed to a different amino acid profile, peptides of different types and sizes, and the presence of microelements. The amino acid profile of the peptones was determined by UHPLC (Supporting Information) and revealed significant differences in the amino acid content of each of the peptones, which might influence the metabolism of the fungus. Moreover, not only the amino acid profile but the total percentage of amino acids were different (84%, 94%, and 66% for meat, casein, and soybean peptones, respectively), which directly impacts the protein synthesis of the microorganism.[42] For these reasons, it is difficult to establish a relationship between a nitrogen source and the synthesis of certain enzymes. Further studies on a genetic level may provide valuable information.[43]

Optimization of Glucose and Peptone Concentration in the Media through Response Surface Methodology. Glucose and peptone concentrations were selected as variables due to their strong influence on the metabolism of filamentous fungi.[36] The selection of the variable ranges is one of the most critical points in any optimization study and highly depends on the process studied. Due to the capability of *F. culmorum* to reduce and oxidize HMF, widely spread points within the common values of both nutrients in microbiological media were first selected to get an overview of the design space. It is worth mentioning that the strategy employed in the sequential development of any model highly depends on the nature of the response system, and it should be adapted to every situation. Therefore, a 2^2 factorial design was first performed to study the effects of glucose and peptone concentration over DFF production (Table 2, runs 1−4).

Table 2. Full Factorial Design Augmented with the Central Point

	Coded levels		Real values		Response
Run	Peptones	Glucose	[Peptones] (g/L)	[Glucose] (g/L)	DFF yield (%)
1	1	1	15	34	51.69
2	1	−1	15	6	0
3	−1	1	3	34	0
4	−1	−1	3	6	0
5	0	0	9	20	67.06
6	0	0	9	20	71.76
7	0	0	9	20	75.04
8	0	0	9	20	60.65
9	0	0	9	20	81.82

There was DFF production only for the high level of both variables, with a yield of 52%. DHMF was also produced with a lower yield (26%). The other combinations of the variables yielded DHMF exclusively with high yields (Supporting Information). This indicated that peptone from casein only induced the oxidation into DFF under certain conditions. Further increases of the concentration of both nutrients above the higher levels (15 g/L of peptones and 34 g/L of glucose) were not considered due to the high cost implied and the unrealistic approach it would pose. Instead, a study within the ranges selected was evaluated, taking into account that the objective is not only to maximize the DFF yield but to do it at the lowest cost possible. One of the limitations of two-level factorial designs is the assumption of linearity in the factor effects. Adding a central point to the 2^2 design can overcome that by allowing the estimation of curvature from second-order effects.[30] Therefore, the design was augmented by including the central point performed in quintuplicate, as shown in Table 2 (runs 5−9).

After fitting a first-order model to the data, the lack of fit was highly significant ($p < 0.001$), indicating that something was missing in the model. Furthermore, the data suggested strong evidence for curvature in the region studied. One way to assess the presence of quadratic curvature is by calculating the difference between Y_f and Y_c, being Y_f the average of the runs at the factorial points (Table 2, runs 1−4) and Y_c the average of the center point runs (Table 2, runs 5−9). The largest this value is, the more evidence there is for quadratic curvature in the model.[30] In this case, $Y_f - Y_c = -58.35$, a value large enough to suggest the presence of quadratic effects. This indicated that the optimum was somewhere within the region considered in the first linear model, and there was no need to increase the concentration of both nutrients further.

First Central Composite Design. The findings suggested that augmentation of the design to allow the fitting of a complete second-order model would be useful. The model was augmented by the addition of axial runs ($\alpha = 1.41$), transforming it into a rotatable central composite design (Table 3). This allowed the fitting of a complete second-order model and efficient estimation of pure quadratic terms. The information about the model can be found in the Supporting Information. Overall, it satisfied all the model adequacy checking while being statistically significant.

Several conditions gave a response value of 0, suggesting that the design space may have been too ample, and therefore, most of the factorial and axial points resided far away from the optimum. Despite that, the model allowed a visual interpretation of the data that gave an overview of the oxidation process within the wide region studied (Figure 2), identifying a region of interest containing the optimum where the subsequent experimentation should take place (Figure 2a).

Results indicated that the oxidation capability of *F. culmorum* was highly affected by the concentration of glucose and peptone in the growth medium. Both nutrients must be at specific concentrations for the oxidation to occur with high yields. The reductive pathway was favored above or below these concentrations, and DHMF was produced (Supporting Information), while DFF yields decreased drastically. This indicated strong evidence of curvature within the region studied, which was in concordance with the excellent fit of the quadratic model.

The model was good at estimating the curvature shown by both variables and locating the region of interest, but it

https://doi.org/10.1021/acssuschemeng.1c05308
ACS Sustainable Chem. Eng. 2021, 9, 14550−14558

Table 3. Experimental Design and Responses of the First Central Composite Design

	Coded levels		Real values		Response	
Run	Peptone	Glucose	[Peptone] (g/L)	[Glucose] (g/L)	DFF yield$_{observed}$ (%)	DFF yield$_{predicted}$ (%)
1	1	1	15	34	51.69	45.28
2	1	−1	15	6	0	6.49
3	−1	1	3	34	0	−8.79
4	−1	−1	3	6	0	4.11
5	0	0	9	20	67.06	71.26
6	0	0	9	20	71.76	71.26
7	0	0	9	20	75.04	71.26
8	0	0	9	20	60.65	71.26
9	0	0	9	20	81.82	71.26
10	1.41	0	17.5	20	43.24	42.70
11	−1.41	0	0.5	20	0	2.84
12	0	1.41	9	39.8	0	10.28
13	0	−1.41	9	0.2	0	−7.99

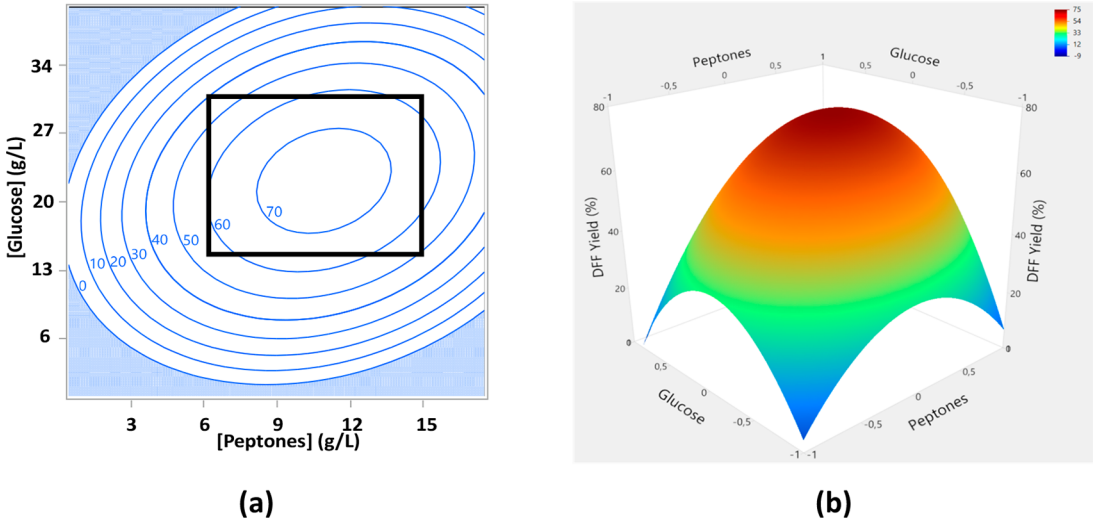

Figure 2. Contour plot (a) and surface plot (b) of the first central composite design. The region of interest selected for further experimentation is squared.

Table 4. Experimental Design and Responses of the Second Central Composite Design

	Coded levels		Real values		Response	
Run	Peptone	Glucose	[Peptone] (g/L)	[Glucose] (g/L)	DFF yield$_{observed}$ (%)	DFF yield$_{predicted}$ (%)
1	0	0	10.5	22	80.28	86.32
2	0	−1.41	10.5	14.9	82.48	84.17
3	0	1.41	10.5	29.1	42.14	43.15
4	1	1	13.5	27	86.78	86.90
5	0	0	10.5	22	90.84	86.32
6	−1.41	0	6.3	22	17.94	21.02
7	0	0	10.5	22	86.96	86.32
8	1	−1	13.5	17	67.92	67.55
9	−1	−1	7.5	17	77.85	75.04
10	−1	1	7.5	27	0	−2.33
11	1.41	0	14.7	22	79.22	78.83
12	0	0	10.5	22	87.40	86.32
13	0	0	10.5	22	86.10	86.32

provided little information about the optimum. The ranges selected for both variables were too widespread, and extreme responses were observed (note that only three of the nine conditions assayed yielded DFF). Moreover, the maximum yields predicted by the model were not optimal (74.1% ± 9.7%). The results manifested the need for further optimization to determine how sensitive the response was when moving within the region of interest containing the estimated optimum, therefore obtaining more information about the process and, hopefully, a better estimation of the optimum conditions. Due to the evidence of curvature provided, a second quadratic model was built around the

https://doi.org/10.1021/acssuschemeng.1c05308
ACS Sustainable Chem. Eng. 2021, 9, 14550−14558

Table 5. ANOVA of the Second Central Composite Design

Source	Sum of squares	DF	Mean square	*F*-ratio	Prob > *F*
Model	10233.995	5	2046.80	167.5672	<0.0001
[Peptone] (x_1)	3341.5097	1	3341.5097	273.5625	<0.0001
[Glucose] (x_2)	1682.9611	1	1682.9611	137.7805	<0.0001
$x_1 \times x_2$	2338.4825	1	2338.4825	191.4467	<0.0001
$x_1 \times x_1$	2303.3001	1	2303.3001	188.5664	<0.0001
$x_2 \times x_2$	893.0352	1	893.0352	73.1109	<0.0001
Error	85.504	7	12.21		
Lack of fit	26.9934	3	8.9978	0.6151	0.6405
Pure error	58.5101	4	14.6275		

R^2 = 0.9917; $R^2_{adjusted}$ = 0.9857; $R^2_{predicted}$: 0.9725

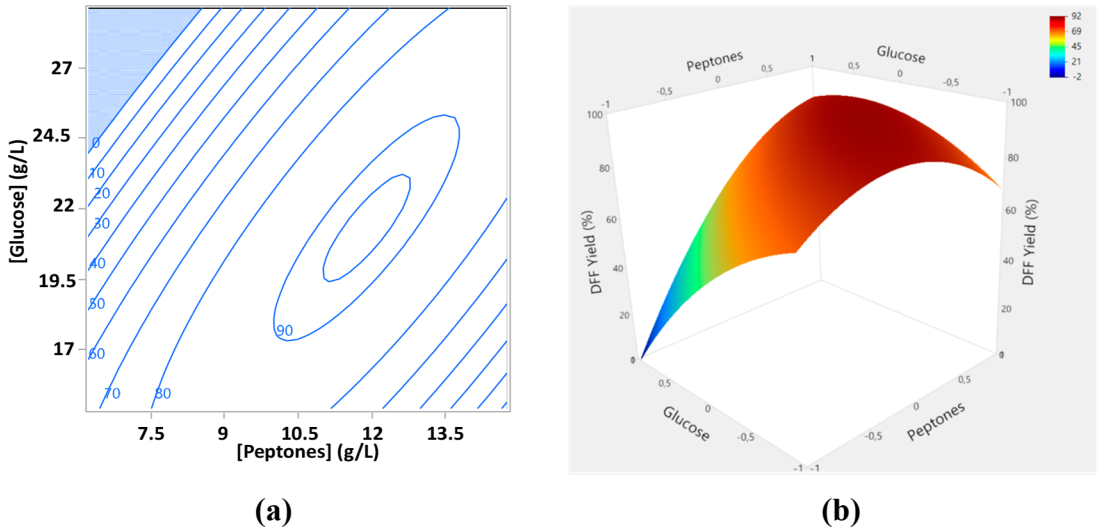

Figure 3. Contour plot (a) and surface plot (b) of the second central composite design.

region of interest, highlighted in Figure 2a, establishing a smaller design space within the one used in the first model.

Second Central Composite Design. A randomized rotatable central composite design was performed. The central point and the ranges of the variables were selected according to the information obtained from the first model. Therefore, the parts of the design space that corresponded to suboptimal responses were discarded, and the new design space was built around the optimum previously found. The maximum DFF yield was generally observed at 48 h for the different conditions (Supporting Information), and therefore, the analysis was performed at that time. Table 4 shows the experimental design, responses observed, and responses predicted by the model.

Analysis of variance (ANOVA) is presented in Table 5. The model explained 98.57% of the variability in the data, and we could expect the model to explain 97.25% of the variability in predicting new observations.

The *p*-value for the model was less than 0.05, indicating that it was statistically significant, while the lack of fit was statistically insignificant (p = 0.6405). The concentration of peptone and glucose, the interaction between both variables, and the quadratic effects were highly significant (p < 0.0001). Therefore, both the concentration of peptone and glucose showed curvature evidence in the response within the design space. The fitted second-order response function in terms of coded variables is

$$\text{DFF Yield (\%)} = 86.32 + 20.44x_1 - 14.50x_2 - 18.20x_1^2 - 11.33x_2^2 + 24.18x_1x_2 \quad (2)$$

where the negative signs of the regression coefficients for the quadratic terms indicate the existence of a local maximum within the design space, and the magnitude of the coefficients is proportional to their effects.

Results displayed in Figure 3 confirm that the oxidation capability of *F. culmorum* was highly affected by the concentration of glucose and peptone in the media. It is worth noting that the contour plot of the second model (Figure 3a) differs from the same region within the first model (Figure 2a). This reinforced the previous hypothesis that the first model provided little information about the optimum, although it successfully located the region of interest. Interestingly, the visual results suggest that high yields come from a certain ratio between glucose and peptone concentration. Peptone and glucose are known to be some of the most expensive ingredients of culture media. Therefore, the results obtained were useful because besides estimating the optimum conditions, they estimate the minimum amount of both nutrients that gives satisfactory enough yields, reducing the cost of the process.

Validation of the Model. Although RSM models are usually validated only at the optimum conditions, the accuracy of the model's predictions within different regions of the design space was considered of interest. Therefore, the model was validated by running independent assays at the optimum

https://doi.org/10.1021/acssuschemeng.1c05308
ACS Sustainable Chem. Eng. 2021, 9, 14550−14558

Table 6. Validation of the Second Central Composite Design[a]

	Coded levels		Real values			
Run	Peptone	Glucose	[Peptone] (g/L)	[Glucose] (g/L)	Predicted yield (%)	Observed yield (%)
1[c]	0.47	−0.14	11.9	21.3	92.12	92.08 ± 4.30
2	0.5	0.5	12	24.5	87.95	90.04 ± 0.21
3	0	−1	10.5	17	89.49	86.63 ± 0.50
4	−0.2	−0.2	9.9	21	84.92	86.40[b]
5	−1.35	−1	6.3	27	≤0	0
6	−0.5	−0.4	9	29	80.38	71.27 ± 8.00

[a]Conditions: 50 mM HMF, three discs of biocatalyst, pH 5.25, 160 rpm, and 28 °C. [b]Sample loss. [c]Optimum conditions.

point (Table 6, run 1) at three selected points within the design space where the predicted DFF yields were higher than 80% (Table 6, runs 2−3−4) and at one point where the predicted yield was ≤0 (Table 6, run 5). In addition, the central point from the first model, which was within the design space, was also considered (Table 6, run 6).

The predictions made by the model were highly accurate for the optimum (Table 6, run 1) and most of the other conditions evaluated (Table 6, runs 2−5), with errors less than 5%. For run 6, the yields were slightly overestimated, arguably due to the high variability observed among the repetitions. Nevertheless, the validation was satisfactory considering the innate variability between independent assays when working with whole cells. Moreover, it confirmed that there was a wide range of conditions in which high yields (>85%) were obtained. Figure 4 shows the concentration of the different

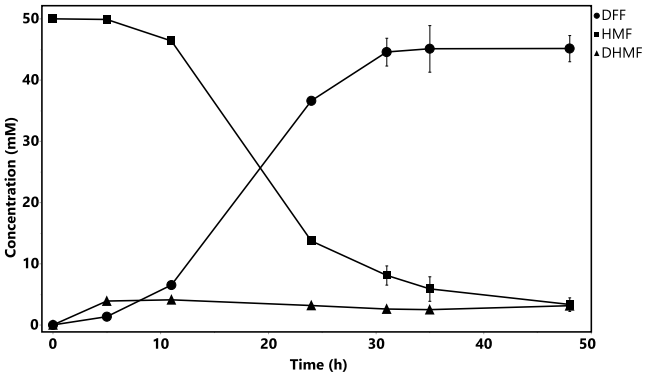

Figure 4. Reaction profile under the optimum conditions. Conditions: 50 mM HMF, 15 mL of medium (20 g/L of malt extract, 21.3 g/L of glucose, 11.9 g/L of peptones), three discs of biocatalyst, pH 5.25, 160 rpm, and 28 °C.

compounds during the reaction under the optimum conditions. Interestingly, there was some DHMF production within the first 6 h of the reaction that remained at a low concentration until high concentrations of DFF were quantified within 31 h, leading to a high yield (92%), selectivity (94%), and productivity (4.4 g/(L·d)). Moreover, DFF was stable in time as no significant differences were observed at 48 h. This indicated that DFF was not further oxidized to the corresponding acids by *F. culmorum*, making it an interesting biocatalyst for DFF production. DFF was successfully recovered from the reaction broth with a recovery yield greater than 90% as a brown solid. The NMR of the crude product was almost identical to that of the commercial standard (Supporting Information).

Toxicity of HMF and DFF toward the Cells. The toxicity level of HMF toward the cells was assessed by increasing the initial concentration of HMF added to the media up to 100 mM (Supporting Information). There was a decrease in the DFF yield when the initial concentration of HMF added was higher than 50 mM, achieving a DFF yield of 70% and 40% within 48 h for concentrations of HMF of 75 and 100 mM, respectively. A fed-batch approach was considered to overcome the toxic effect, in which 50 mM HMF was added again once the substrate was metabolized entirely (Supporting Information). However, there was no further transformation of the HMF added in the second cycle, suggesting that the toxicity level of DFF toward the cells is also around 50 mM under the conditions studied. Different approaches can be taken to overcome the toxic effect, such as increasing the inoculum size of the cells by adding more discs or the inoculation in the form of spores.[22] To that end, the inoculation of the fungus from a suspension of spores was assessed. However, there was HMF reduction to DHMF with high yields (data not shown), indicating that the way of inoculation of the fungus has a significant effect on the HMF biotransformation. Another possibility that is currently being considered is to perform a biphasic system with a solvent that separates the DFF produced from the media. Further work considering these alternatives would improve the process performance and efficiency.

Although several results have been reported in the enzymatic synthesis of DFF from HMF, the low productivities obtained manifest the need for further investigation. Moreover, the combination of different enzymes, which are usually produced and purified separately in different hosts, is needed to achieve a high yield and selectivity,[15,16,44] adding a high cost to the process. *F. culmorum* shows the capability to reduce to DHMF and oxidize to DFF high concentrations of HMF, depending on media conditions. The enzymes that catalyze the reduction of HMF to DHMF when using whole cells are described in various microorganisms. For instance, Martins et al.[46] and Ran et al.[45] hypothesized that an aldehyde oxidoreductase is responsible for the reduction in the filamentous fungi *Aspergillus nidulans* and the fungi *Pleurotus ostreatus*, respectively. However, the whole-cell oxidation of HMF to DFF has not been described to the best of our knowledge. *Fusarium* species are natural producers of the enzyme GO,[23,24] which catalyzes the oxidation of HMF to DFF with quantitative yields in combination with catalase and HRP.[15,16] Arguably, *F. culmorum* can produce the enzymes needed for the efficient oxidation of HMF to DFF, but their expression is highly dependent on the nitrogen source and the peptone and glucose concentrations in the media.

Hybrid processes, understood as the combination of different biocatalytic approaches (fermentation, microbial catalysis, and enzyme catalysis) provide hope in the biocatalytic sustainable transformation of substrates like

https://doi.org/10.1021/acssuschemeng.1c05308
ACS Sustainable Chem. Eng. 2021, 9, 14550−14558

HMF.[21] Therefore, the novel process presented could also be used as an intermediate step in the synthesis of other HMF derivatives (such as FDCA) produced through further oxidation of DFF.

CONCLUSIONS

Herein, we describe the whole-cell oxidation of HMF to DFF for the first time to the best of our knowledge. The use of a single whole-cell catalyst to produce DFF represents a significant advance thanks to the inherent presence of all the enzymes required, reducing the cost of the process. The nitrogen source and the concentration of peptone and glucose in the reaction media highly influenced the transformation of HMF by the strain of *F. culmorum* EAN 51. The concentration of both nutrients was optimized through RSM, allowing DFF production with a high yield (92%) and selectivity (94%) starting from 50 mM HMF under the estimated optimum conditions. Moreover, the RSM study provided a better understanding of the conditions needed to efficiently oxidize HMF, which could be of interest for further optimization of the reaction. The knowledge acquired may not be limited to the biocatalyst and process used. Furthermore, the process described meets several principles of green chemistry: there is no use or generation of toxic substances, the solvents and auxiliaries used are safe, it is conducted at ambient temperature and pressure, the substrate and the biocatalyst come from renewable feedstocks, there is no use of derivatives, the biocatalyst is highly selective and biodegradable, and it is performed under mild and safe conditions. Finally, DFF can be isolated from the broth yielding a crude final product similar to the commercial one. These results open a new line of investigation in the sustainable production of DFF from renewable biobased resources.

ASSOCIATED CONTENT

Supporting Information

The Supporting Information is available free of charge at https://pubs.acs.org/doi/10.1021/acssuschemeng.1c05308.

Additional information including amino acid profile of the peptones, data related to the RSM, ^{1}H NMR of the recovered DFF, and toxicity levels of HMF and DFF toward the cells (PDF)

AUTHOR INFORMATION

Corresponding Authors

Alberto Millán Acosta − *Chemistry Department, University of Lleida, 25198 Lleida, Spain*; Email: alberto.millan@udl.cat

Ramon Canela-Garayoa − *Chemistry Department, University of Lleida, 25198 Lleida, Spain*; orcid.org/0000-0003-1095-6607; Email: ramon.canela@udl.cat

Authors

Clara Cuesta Turull − *Chemistry Department, University of Lleida, 25198 Lleida, Spain*

Diana Cosovanu − *Chemistry Department, University of Lleida, 25198 Lleida, Spain*

Núria Sala Martí − *Food Technology Department, University of Lleida, 25198 Lleida, Spain*

Complete contact information is available at: https://pubs.acs.org/10.1021/acssuschemeng.1c05308

Funding

This work was partially supported by the Spanish Government (PID2019-110735RB-C21, MICIN/FEDER) and the Catalan Government (FI_B1_00135).

Notes

The authors declare no competing financial interest.

ACKNOWLEDGMENTS

The authors would like to thank the Catalan Government for the quality accreditation given to their research group 2017 SGR 828. A.M.A would like to thank "Generalitat de Catalunya" for the Grant FI Agaur. C.C.T. would like to thank "Universitat de Lleida" for the grant "Beca d'introducció a la recerca". D.C. would like to thank "Universitat de Lleida" for the grant "Ajuts per a personal predoctoral de la UdL". The graphical abstract was created with BioRender.com.

REFERENCES

(1) Liguori, R.; Amore, A.; Faraco, V. Waste Valorization by Biotechnological Conversion into Added Value Products. *Appl. Microbiol. Biotechnol.* **2013**, *97* (14), 6129−6147.

(2) Van Putten, R. J.; Van Der Waal, J. C.; De Jong, E.; Rasrendra, C. B.; Heeres, H. J.; De Vries, J. G. Hydroxymethylfurfural, a Versatile Platform Chemical Made from Renewable Resources. *Chem. Rev.* **2013**, *113* (3), 1499−1597.

(3) Zhang, Y.; Zhang, J.; Su, D. 5-Hydroxymethylfurfural: A Key Intermediate for Efficient Biomass Conversion. *J. Energy Chem.* **2015**, *24* (5), 548−551.

(4) Hu, L.; He, A.; Liu, X.; Xia, J.; Xu, J.; Zhou, S.; Xu, J. Biocatalytic Transformation of 5-Hydroxymethylfurfural into High-Value Derivatives: Recent Advances and Future Aspects. *ACS Sustainable Chem. Eng.* **2018**, *6* (12), 15915−15935.

(5) Ma, J.; Du, Z.; Xu, J.; Chu, Q.; Pang, Y. Efficient Aerobic Oxidation of 5-Hydroxymethylfurfural to 2,5-Diformylfuran, and Synthesis of a Fluorescent Material. *ChemSusChem* **2011**, *4* (1), 51−54.

(6) Hopkins, K. T.; Wilson, W. D.; Bender, B. C.; McCurdy, D. R.; Hall, J. E.; Tidwell, R. R.; Kumar, A.; Bajic, M.; Boykin, D. W. Extended Aromatic Furan Amidino Derivatives as Anti-*Pneumocystis Carinii* Agents. *J. Med. Chem.* **1998**, *41* (20), 3872−3878.

(7) Amarasekara, A. S.; Green, D.; Williams, L. T. D. Renewable Resources Based Polymers: Synthesis and Characterization of 2,5-Diformylfuran-Urea Resin. *Eur. Polym. J.* **2009**, *45* (2), 595−598.

(8) Domínguez de María, P.; Guajardo, N. Biocatalytic Valorization of Furans: Opportunities for Inherently Unstable Substrates. *ChemSusChem* **2017**, *10* (21), 4123−4134.

(9) Peyrton, J.; Avérous, L. Aza-Michael Reaction as a Greener, Safer, and More Sustainable Approach to Biobased Polyurethane Thermosets. *ACS Sustainable Chem. Eng.* **2021**, *9*, 4872−4884.

(10) Kucherov, F. A.; Romashov, L. V.; Galkin, K. I.; Ananikov, V. P. Chemical Transformations of Biomass-Derived C6-Furanic Platform Chemicals for Sustainable Energy Research, Materials Science, and Synthetic Building Blocks. *ACS Sustainable Chem. Eng.* **2018**, *6* (7), 8064−8092.

(11) Yan, Y.; Li, K.; Zhao, J.; Cai, W.; Yang, Y.; Lee, J. M. Nanobelt-Arrayed Vanadium Oxide Hierarchical Microspheres as Catalysts for Selective Oxidation of 5-Hydroxymethylfurfural toward 2,5-Diformylfuran. *Appl. Catal., B* **2017**, *207*, 358−365.

(12) Zhao, J.; Chen, X.; Du, Y.; Yang, Y.; Lee, J. M. Vanadium-Embedded Mesoporous Carbon Microspheres as Effective Catalysts for Selective Aerobic Oxidation of 5-Hydroxymethyl-2-Furfural into 2,5-Diformylfuran. *Appl. Catal., A* **2018**, *568* (July), 16−22.

(13) Zhao, J.; Jayakumar, A.; Hu, Z. T.; Yan, Y.; Yang, Y.; Lee, J. M. MoO3-Containing Protonated Nitrogen Doped Carbon as a Bifunctional Catalyst for One-Step Synthesis of 2,5-Diformylfuran from Fructose. *ACS Sustainable Chem. Eng.* **2018**, *6* (1), 284−291.

(14) Zhao, J.; Yan, Y.; Hu, Z. T.; Jose, V.; Chen, X.; Lee, J. M. Bifunctional Carbon Nanoplatelets as Metal-Free Catalysts for Direct Conversion of Fructose to 2,5-Diformylfuran. *Catal. Sci. Technol.* **2020**, *10* (13), 4179−4183.
(15) Qin, Y. Z.; Li, Y. M.; Zong, M. H.; Wu, H.; Li, N. Enzyme-Catalyzed Selective Oxidation of 5-Hydroxymethylfurfural (HMF) and Separation of HMF and 2,5-Diformylfuran Using Deep Eutectic Solvents. *Green Chem.* **2015**, *17* (7), 3718−3722.
(16) Wu, Z.; Shi, L.; Yu, X.; Zhang, S.; Chen, G. Co-Immobilization of Tri-Enzymes for the Conversion of Hydroxymethylfurfural to 2,5-Diformylfuran. *Molecules* **2019**, *24* (20), 3648.
(17) Kadowaki, M.; Godoy, M.; Kumagai, P.; Costa-Filho, A.; Mort, A.; Prade, R.; Polikarpov, I. Characterization of a New Glyoxal Oxidase from the Thermophilic Fungus *Myceliophthora Thermophila* M77: Hydrogen Peroxide Production Retained in 5-Hydroxymethyl-furfural Oxidation. *Catalysts* **2018**, *8* (10), 476.
(18) Mathieu, Y.; Offen, W. A.; Forget, S. M.; Ciano, L.; Viborg, A. H.; Blagova, E.; Henrissat, B.; Walton, P. H.; Davies, G. J.; Brumer, H. Discovery of a Fungal Copper Radical Oxidase with High Catalytic Efficiency toward 5-Hydroxymethylfurfural and Benzyl Alcohols for Bioprocessing. *ACS Catal.* **2020**, *10* (5), 3042−3058.
(19) Wachtmeister, J.; Rother, D. Recent Advances in Whole Cell Biocatalysis Techniques Bridging from Investigative to Industrial Scale. *Curr. Opin. Biotechnol.* **2016**, *42*, 169−177.
(20) de Carvalho, C. C. Whole Cell Biocatalysts: Essential Workers from Nature to the Industry. *Microb. Biotechnol.* **2017**, *10* (2), 250−263.
(21) Woodley, J. M. Towards the Sustainable Production of Bulk-Chemicals Using Biotechnology. *New Biotechnol.* **2020**, *59* (April), 59−64.
(22) Millán, A.; Sala, N.; Torres, M.; Canela-Garayoa, R. Biocatalytic Transformation of 5-Hydroxymethylfurfural into 2,5-Di-(Hydroxymethyl)Furan by a Newly Isolated Fusarium Striatum Strain. *Catalysts* **2021**, *11* (2), 216.
(23) Paukner, R.; Staudigl, P.; Choosri, W.; Haltrich, D.; Leitner, C. Expression, Purification, and Characterization of Galactose Oxidase of *Fusarium Sambucinum* in *E. Coli*. *Protein Expression Purif.* **2015**, *108*, 73−79.
(24) Gasparotto, E. P. L.; Abrão, S. C. C.; Inagaki, S. Y.; Tessmann, D. J.; Kemmelmeier, C.; Tessmann, I. P. B. Production and Characterization of Galactose Oxidase Produced by Four Isolates of *Fusarium Graminearum*. *Braz. Arch. Biol. Technol.* **2006**, *49* (4), 557−564.
(25) Zeng, Y. J.; Yang, H. R.; Wu, X. L.; Peng, F.; Huang, Z.; Pu, L.; Zong, M. H.; Yang, J. G.; Lou, W. Y. Structure and Immunomodulatory Activity of Polysaccharides from *Fusarium Solani* DO7 by Solid-State Fermentation. *Int. J. Biol. Macromol.* **2019**, *137*, 568−575.
(26) Pessôa, M. G.; Paulino, B. N.; Mano, M. C. R.; Neri-Numa, I. A.; Molina, G.; Pastore, G. M. *Fusarium* Species—a Promising Tool Box for Industrial Biotechnology. *Appl. Microbiol. Biotechnol.* **2017**, *101* (9), 3493−3511.
(27) Alaeddini, A.; Yang, K.; Mao, H.; Murat, A.; Ankenman, B. An Adaptive Sequential Experimentation Methodology for Expensive Response Surface Optimization - Case Study in Traumatic Brain Injury Modeling. *Qual. Reliab. Eng. Int.* **2014**, *30* (6), 767−793.
(28) Gundogdu, T. K.; Deniz, I.; Caliskan, G.; Sahin, E. S.; Azbar, N. Experimental Design Methods for Bioengineering Applications. *Crit. Rev. Biotechnol.* **2016**, *36* (2), 368−388.
(29) Toms, D.; Deardon, R.; Ungrin, M. Climbing the Mountain: Experimental Design for the Efficient Optimization of Stem Cell Bioprocessing. *J. Biol. Eng.* **2017**, *11* (1), 1−11.
(30) Myers, R. H.; Mongomery, D. C.; Anderson-Cook, C. M. *Response Surface Methodology: Process and Product Optimization Using Designed Experiments*, 3rd ed.; John Wiley & Sons, Ltd.: Hoboken, NJ, 2009.
(31) Yolmeh, M.; Jafari, S. M. Applications of Response Surface Methodology in the Food Industry Processes. *Food Bioprocess Technol.* **2017**, *10* (3), 413−433.
(32) Singh, V.; Haque, S.; Niwas, R.; Srivastava, A.; Pasupuleti, M.; Tripathi, C. K. M. Strategies for Fermentation Medium Optimization: An in-Depth Review. *Front. Microbiol.* **2017**, *7*, 2087.
(33) Colgrave, M. L.; Allingham, P. G.; Jones, A. Hydroxyproline Quantification for the Estimation of Collagen in Tissue Using Multiple Reaction Monitoring Mass Spectrometry. *J. Chromatogr. A* **2008**, *1212* (1−2), 150−153.
(34) Dai, Z.; Wu, Z.; Jia, S.; Wu, G. Analysis of Amino Acid Composition in Proteins of Animal Tissues and Foods as Pre-Column o-Phthaldialdehyde Derivatives by HPLC with Fluorescence Detection. *J. Chromatogr. B: Anal. Technol. Biomed. Life Sci.* **2014**, *964*, 116−127.
(35) Guo, S.; Duan, J. A.; Qian, D.; Tang, Y.; Qian, Y.; Wu, D.; Su, S.; Shang, E. Rapid Determination of Amino Acids in Fruits of *Ziziphus Jujuba* by Hydrophilic Interaction Ultra-High-Performance Liquid Chromatography Coupled with Triple-Quadrupole Mass Spectrometry. *J. Agric. Food Chem.* **2013**, *61* (11), 2709−2719.
(36) Papagianni, M. Fungal Morphology and Metabolite Production in Submerged Mycelial Processes. *Biotechnol. Adv.* **2004**, *22* (3), 189−259.
(37) Alberton, D.; Silva de Oliveira, L.; Peralta, R. M.; Barbosa-Tessmann, I. P. Production, Purification, and Characterization of a Novel Galactose Oxidase from Fusarium Acuminatum. *J. Basic Microbiol.* **2007**, *47* (3), 203−212.
(38) Caridis, K. A.; Christakopoulos, P.; Macris, B. J. Simultaneous Production of Glucose Oxidase and Catalase by Alternaria Alternata. *Appl. Microbiol. Biotechnol.* **1991**, *34* (6), 794−797.
(39) Li, Y. M.; Zhang, X. Y.; Li, N.; Xu, P.; Lou, W. Y.; Zong, M. H. Biocatalytic Reduction of HMF to 2,5-Bis(Hydroxymethyl)Furan by HMF-Tolerant Whole Cells. *ChemSusChem* **2017**, *10* (2), 372−378.
(40) Xu, Z.-H.; Cheng, A.-D.; Xing, X.-P.; Zong, M.-H.; Bai, Y.-P.; Li, N. Improved Synthesis of 2,5-Bis(Hydroxymethyl)Furan from 5-Hydroxymethylfurfural Using Acclimatized Whole Cells Entrapped in Calcium Alginate. *Bioresour. Technol.* **2018**, *262* (April), 177−183.
(41) He, Y. C.; Jiang, C. X.; Chong, G. G.; Di, J. H.; Ma, C. L. Biological Synthesis of 2,5-Bis(Hydroxymethyl)Furan from Biomass-Derived 5-Hydroxymethylfurfural by *E. Coli* CCZU-K14 Whole Cells. *Bioresour. Technol.* **2018**, *247*, 1215−1220.
(42) Pasupuleti, V. K.; Demain, A. L. *Protein Hydrolysates in Biotechnology*; Springer, 2010. DOI: 10.1007/978-1-4020-6674-0.
(43) Wiame, J. M.; Grenson, M.; Ars, H. N. Nitrogen Catabolite Repression in Yeasts and Filamentous Fungi. *Adv. Microb. Physiol.* **1985**, *26* (C), 1−88.
(44) Cajnko, M. M.; Novak, U.; Grilc, M.; Likozar, B. Enzymatic Conversion Reactions of 5-Hydroxymethylfurfural (HMF) to Bio-Based 2,5-Diformylfuran (DFF) and 2,5-Furandicarboxylic Acid (FDCA) with Air: Mechanisms, Pathways and Synthesis Selectivity. *Biotechnol. Biofuels* **2020**, *13* (1), 1−11.
(45) Ran, H.; Zhang, J.; Gao, Q.; Lin, Z.; Bao, J. Analysis of Biodegradation Performance of Furfural and 5-Hydroxymethylfurfural by *Amorphotheca Resinae* ZN1. *Biotechnol. Biofuels* **2014**, *7*, 51.
(46) Martins, C.; Hartmann, D. O.; Varela, A.; Coelho, J. A. S.; Lamosa, P.; Afonso, C. A. M.; Silva Pereira, C. Securing a Furan-based Biorefinery: Disclosing the Genetic Basis of the Degradation of Hydroxymethylfurfural and Its Derivatives in the Model Fungus *Aspergillus Nidulans*. *Microb. Biotechnol.* **2020**, *13* (6), 1983−1996.

https://doi.org/10.1021/acssuschemeng.1c05308
ACS Sustainable Chem. Eng. 2021, 9, 14550−14558